energies

Article

The Probabilistic Optimal Integration of Renewable Distributed Generators Considering the Time-Varying Load Based on an Artificial Gorilla Troops Optimizer

Ashraf Ramadan [1], Mohamed Ebeed [2], Salah Kamel [1], Ahmed M. Agwa [3,4,*] and Marcos Tostado-Véliz [5,*]

[1] Department of Electrical Engineering, Aswan University, Aswan 81542, Egypt; ashraframadanragab@gmail.com (A.R.); skamel@aswu.edu.eg (S.K.)
[2] Faculty of Engineering, Sohag University, Sohag 82524, Egypt; mebeed@eng.sohag.edu.eg
[3] Department of Electrical Engineering, College of Engineering, Northern Border University, Arar 1321, Saudi Arabia
[4] Prince Faisal bin Khalid bin Sultan Research Chair in Renewable Energy Studies and Applications (PFCRE), Northern Border University, Arar 1321, Saudi Arabia
[5] Department of Electrical Engineering, University of Jaén, 23700 EPS Linares, Spain
* Correspondence: ah1582009@yahoo.com (A.M.A.); mtostado@ujaen.es (M.T.-V.)

check for updates

Citation: Ramadan, A.; Ebeed, M.; Kamel, S.; Agwa, A.M.; Tostado-Véliz, M. The Probabilistic Optimal Integration of Renewable Distributed Generators Considering the Time-Varying Load Based on an Artificial Gorilla Troops Optimizer. *Energies* **2022**, *15*, 1302. https://doi.org/10.3390/en15041302

Academic Editor: Andrea De Pascale

Received: 20 January 2022
Accepted: 8 February 2022
Published: 11 February 2022

Abstract: Renewable distributed generators (RDGs) are widely embedded in electrical distribution networks due to their economic, technological, and environmental benefits. However, the main problem with RDGs, photovoltaic generators, and wind turbines, in particular, is that their output powers are constantly changing due to variations in sun irradiation and wind speed, leading to power system uncertainty. Such uncertainties should be taken into account when selecting the optimal allocation of RDGs. The main innovation of this paper is a proposed efficient metaheuristic optimization technique for the sizing and placement of RDGs in radial distribution systems considering the uncertainties of the loading and RDG output power. A Monte Carlo simulation method, along with the backward reduction algorithm, is utilized to create a set of scenarios to model these uncertainties. To find the positions and ratings of the RDGs, the artificial gorilla troops optimizer (GTO), a new efficient strategy that minimizes the total cost, is used to optimize a multiobjective function, total emissions, and total voltage deviations, as well as the total voltage stability boosting. The proposed technique is tested on an IEEE 69-bus network and a real Egyptian distribution grid (East Delta Network (EDN) 30-bus network). The results indicate that the proposed GTO can optimally assign the positions and ratings of RDGs. Moreover, the integration of RDGs into an IEEE 69-bus system can reduce the expected costs, emissions, and voltage deviations by 28.3%, 52.34%, and 66.95%, respectively, and improve voltage stability by 5.6%; in the EDN 30-bus system, these values are enhanced by 25.97%, 51.1%, 67.25%, and 7.7%, respectively.

Keywords: renewable energy; solar; wind; DG; uncertainties; gorilla troops optimizer; radial distribution system; backward reduction methodology; Monte Carlo simulation approach

1. Introduction

Incorporating distributed generators (DGs) can enhance system performance and voltage profiles, reducing both the total production cost of electricity and harmful greenhouse gas emissions. A major factor in determining the appropriate size and location of DGs in electrical systems is uncertainty, which considerably increases the complexity of the problem. The major uncertainty factors in distribution systems are the load demand and the output power of the renewable RDGs, due to variations in solar radiation and the wind speed. Thus, determining the optimal allocation of RDGs in a radial distribution network (RDN) is a strenuous and challenging task.

A lot of published work in this field has been solely focused on DG planning and allocation, and very little research has addressed uncertainty and optimization methodologies at the same time, which is crucial for DG planning. Therefore, the novelty of this study lies in a proposed optimization approach for the DG placement problem, as well as uncertainty methods. The fundamental goal of installing DGs in distribution systems is to ensure optimal distribution network operations by lowering system losses, improving voltage profiles, and increasing system reliability [1]. Due to growing fuel costs, the cost of generating energy with traditional generators is rapidly increasing. In contrast, the cost of renewable energy systems, such as solar photovoltaic (PV) and wind energy, has dropped significantly [2]. In order to reduce the number of scenarios formed by Monte Carlo simulations, a backward reduction algorithm was used [3]. Determining the optimal allocation of DGs provides a number of benefits, including lower energy costs, reduced emissions, and improved voltage profiles [4–6]. Nevertheless, because RDGs are inherently uncertain, the inappropriate placement of DGs can result in system instability and voltage variations [7,8].

A lot of research has analyzed the problem of optimal DG integration from various angles. The authors of [9] used the crow search algorithm to determine the optimal location and size of DGs. A sine cosine algorithm (SCA) was applied in [10] to determine DG allocation and voltage profiles. To resolve the DG integration problem, taking into account RDG generation uncertainty, the authors of [11] proposed combining a Monte Carlo approach with a genetic algorithm. The model considered the cost of DGs, as well as energy losses. In [12], an effective approach called the 'coefficient particle swarm optimization' (CPSO) was used to diminish the total energy losses for sizing and positioning DG units. In [13], using a scenario synthesis approach, optimal power siting and sizing for an active distribution system, considering demand response and the optimal integration of wind turbines (WTs), as well as system uncertainties, were determined using a cuckoo search algorithm.

In [3], the authors employed various bio-inspired methods, such as grey wolf optimization, manta ray foraging optimization, satin bowerbird optimization, and whale optimization (WOA), as well as Monte Carlo simulation, to determine the optimal position of DGs. In [14], an effective algorithm was presented, the equilibrium optimizer, with the purpose of resolving the energy management issue of a microgrid and optimizing DG location and size. In [15], a genetic algorithm was proposed to solve the DG allocation problem, taking into account load and DG uncertainties. The authors of [16] suggested a bilayer optimization technique to achieve optimal battery energy storage systems and to determine the solar photovoltaic (SPV) locations in a distribution system.

In [17], a novel ant lion optimizer (ALO) was presented, which lowered the cost of energy, reduced losses and voltage deviation, and improved reliability. In [18], particle swarm optimization (PSO), using a probabilistic uncertainty modeling technique, was suggested for DG sizing, siting, and DG wind penetration in a distribution system. PSO, modified SCA [19,20], and other approaches have been utilized to define the optimal size and site of DGs in radial distribution systems, while taking system uncertainties into account. In [21], a modified differential evolution algorithm was proposed for optimal DG allocation. In distribution systems, numerous metaheuristic strategies are employed to solve the distributed generators allocation problem. Some of the newest algorithms, such as the artificial hummingbird algorithm (AHA), are discussed in [22]. The gorilla troops optimizer (GTO) is a novel optimization technique that models gorilla social behavior and movement in the wild [23]. The GTO is utilized to solve a range of engineering problems, including extracting various PV models [24]. In this research, the GTO is used to determine optimal wind and solar allocation. An IEEE 69-bus and an EDN 30-bus, as well as an actual network in Egypt, are used as test networks, taking into consideration the uncertainties of load demand, wind, and solar power generators. The contributions and innovation of this paper are summarized as follows:

1. The application of an efficient metaheuristic optimization technique called GTO, to determine the optimal sizes and placement of the RDGs.
2. The allocation problem of RDGs is solved, taking into account the uncertainties of the load and the output power of RDGs.
3. The uncertainties of the system are addressed using the Monte Carlo simulation method along with the backward reduction algorithm.
4. The allocation problem of the RDGs is solved, and the total cost, total emissions, voltage improvements, and system voltage deviations of the IEEE 69-bus and EDN 30-bus are determined.
5. Statistical comparisons are presented between the proposed algorithm and well-known optimization algorithms to verify the effectiveness of the former.

This paper is structured as follows: Section 2 presents the problem formulation, which includes the objective function. Section 3 presents an overview of how to model uncertainty. Section 4 gives a general review of the GTO method. Section 5 summarizes the collected data, and Section 6 presents the conclusions.

2. Studied Objective Functions

A multiobjective function is used in this study. It is important to note that a collection of scenarios is produced while analyzing or modeling the uncertainty of the power system. As a result, these eventualities are addressed while dealing with sizing and siting problems. Moreover, each scenario has its own set of expected values, as displayed in the sections below. This study applies a multiobjective function that includes the following four functions:

2.1. Minimization of Expected Total Cost (ETCost)

ETCost represents the expected value of electrical energy savings at the main substation ($ECost_{Grid}$). The expected cost of the PV units ($ECost_{PV}$) and WT ($ECost_{WT}$) can be expressed as follows:

$$\mathrm{ETCost} = \mathrm{ECost_{Grid}} + \mathrm{ECost_{PV}} + \mathrm{ECost_{WT}} \quad (1)$$

where:

$$\mathrm{ETCost_{Grid}} = \sum_{k=1}^{Ns} \mathrm{ECost_{Grid,k}} = \sum_{k=1}^{Ns} \mathrm{Cost_{Grid,k}} \times \pi_{S,k} \quad (2)$$

$$\mathrm{Cost_{Grid}} = \mathrm{P_{Grid}} \times \mathrm{K_{Grid}} \quad (3)$$

$$\mathrm{ECost_{PV}} = \sum_{k=1}^{Ns} \mathrm{ECost_{PV,k}} = \sum_{k=1}^{Ns} \pi_{Solar,k} \times (a_{PV} + b_{PV} \times PG_{PV}) \quad (4)$$

$$a_{1PV} = \frac{\text{capital}\ \cos t\_PV \times P_{sr} \times Gr}{\text{life time}\_PV \times 8760 \times LF} \quad (5)$$

$$b_{1PV} = \mathrm{Cost\_PV_{O\&M}} + \mathrm{Cost\_PV_{Fuel}} \quad (6)$$

$$\mathrm{ECost_{wind}} = \sum_{k=1}^{Ns} \mathrm{ECost_{wind,k}} = \sum_{k=1}^{Ns} \pi_{wind,k} \times (a_{wind} + b_{wind} \times PG_{wind}) \quad (7)$$

$$a_{2wind} = \frac{\text{capital}\ \cos t\_wind \times P_{wr} \times Gr}{\text{life time}\_wind \times 8760 \times LF} \quad (8)$$

$$b_{2wind} = \mathrm{Cost\_wind_{O\&M}} + \mathrm{Cost\_wind_{Fuel}} \quad (9)$$

where the power of the grid is P_{Grid}, the real power produced by PV is PG_{PV}, the real power produced by WT is PG_{wind}, the rated power of PV unit is P_{sr}, the rated power of WT unit is P_{wr}, Gr is the annual rate of benefits ($/h), the load factor of DGs is LF, and $\pi_{S,k}$, $\pi_{Solar,k}$, $\pi_{wind,k}$ are the probability load demand, solar irradiance, and wind speed of *k-th* interval, respectively.

The yearly PV unit installation cost is a_{1PV}, while the yearly PV unit operation and maintenance (O&M) cost is b_{1PV}. The yearly wind turbine installation cost is a_{2wind} and the annual O&M cost of WT is b_{2wind}. In this study, capital cos t_PV = 3985 $/kW, $Cost\_PV_{O\&M}$ = 0.01207 $/kWh, and $Cost\_PV_{Fuel}$ = 0 $/kWh were selected as the PV cost coefficients. The wind cost coefficients were set as capital cos t_wind = 1822 $/kW, $Cost\_wind_{O\&M}$ = 0.00952 $/kWh, and $Cost\_wind_{Fuel}$ = 0 $/kWh; the life time of WT and PV were designated as 20 years, and K_{Grid} = 0.096 [25].

2.2. Minimization of Expected Total Emissions (ETEmission)

The most significant pollutants resulting from power generation are CO_2, SO_2, and NO_x. The objective function that describes emissions may be mathematically formulated as follows [9]:

$$\text{ETEmission} = \sum_{k=1}^{Ns} \text{EEmission}_k = \sum_{k=1}^{Ns} \pi_{Grid,k} \times E_{Grid,k} \tag{10}$$

$$f_2(x) = \sum_{i=1}^{N_{DG}} E_{DG_i} + E_{Grid} \tag{11}$$

$$E_{DG_i} = \left(CO_2^{DG} + NO_x^{DG} + SO_2^{DG}\right) \times PG_i \tag{12}$$

$$E_{Grid} = \left(CO_2^{Grid} + NO_x^{Grid} + SO_2^{Grid}\right) \times P_{Grid} \tag{13}$$

The SO_2, CO_2, and NO_x emission rates are 11.6 kg/MWh, 2031 kg/MWh, and 5.06 kg/MWh, respectively [26].

2.3. Minimization of Total Expected Voltage Deviations (ETVD)

$$\text{ETVD} = \sum_{k=1}^{Ns} \text{EVD}_k = \sum_{k=1}^{Ns} \pi_{S,k} \times \text{VD}_k \tag{14}$$

where VD is the sum of voltage deviations, which can be represented as follows:

$$\text{VD} = \sum_{h=1}^{n} |V_h - 1| \tag{15}$$

2.4. Improvement of the Expected Total Voltage Stability (ETVSI)

The expected summation of the voltage stability indicators is as follows:

$$\text{ETVSI} = \sum_{k=1}^{Ns} \text{EVSI}_k = \sum_{k=1}^{Ns} \pi_{S,k} \times \text{VSI}_k \tag{16}$$

where:

$$\text{VSI}_n = |V_n|^4 - 4(P_n X_{nm} - Q_n R_{nm})^2 - 4(P_n X_{nm} + Q_n R_{nm})|V_n|^2 \tag{17}$$

2.5. The Multiobjective Function

The objective functions in this work are as follows: expected total cost (ETCost), expected total emissions (ETEmission), expected total voltage deviations (ETVD), and expected total voltage stability index (ETVSI). These functions are considered simultaneously using the weighted sum method as follows:

$$F = \mu_1 F_1 + \mu_2 F_2 + \mu_3 F_3 + \mu_4 F_4 \tag{18}$$

where μ_1, μ_2, μ_3, and μ_4 are the weighting factors, the sum of which must equal 1:

$$|\mu_1| + |\mu_2| + |\mu_3| + |\mu_4| = 1 \tag{19}$$

The normalized objective functions can be expressed in the following way:

$$F_1 = \frac{\mathrm{ETCost}}{\mathrm{ETCost_{base}}} \tag{20}$$

$$F_2 = \frac{\mathrm{ETEmission}}{\mathrm{ETEmission_{base}}} \tag{21}$$

$$F_3 = \frac{\mathrm{ETVD}}{\mathrm{ETVD_{base}}} \tag{22}$$

$$F_4 = \frac{1}{\mathrm{ETVSI}} \tag{23}$$

2.6. Constraints of the System

2.6.1. Equality Constraints

Equality constraints in RDN include the reactive and active power flow, which can be determined as follows:

$$P_{Grid} + \sum_{j=1}^{NPV} P_{PV,i} + \sum_{j=1}^{NWT} P_{WT,i} = \sum_{j=1}^{NT} P_{loss,i} + \sum_{j=1}^{NB} P_{L,i} \tag{24}$$

$$Q_{Grid} + \sum_{i=1}^{NT} Q_{WT,i} = \sum_{i=1}^{NT} Q_{loss,i} + \sum_{i=1}^{NB} Q_{L,i} \tag{25}$$

2.6.2. Inequality Constraints

$$V_{min} \leq V_i \leq V_{max} \tag{26}$$

$$\sum_{i=1}^{NWT} Q_{WT,i} \leq \sum_{i=1}^{NB} Q_{L,i} \tag{27}$$

$$I_n \leq I_{max,\quad n},\ n\ = 1, 2, 3\ldots, NT \tag{28}$$

where V_{min} and V_{max} are the lower and upper voltage limitations, respectively.

3. Uncertainty Modeling

3.1. Modeling of Wind Speed Uncertainty

The Weibull probability density function (PDF) can be used to model wind speed uncertainty [26] as follows:

$$f_v(v) = \left(\frac{\beta}{\alpha}\right)\left(\frac{v}{\alpha}\right)^{(\beta-1)} \exp\left[-\left(\frac{v}{\alpha}\right)^{\beta}\right], 0 \leq v < \infty \tag{29}$$

The Weibull PDF shaping and scaling factors are β, α; these were set at 9.4 and 2.4, respectively. Figure 1 shows a 1000 Monte Carlo wind speed distribution scenario using Weibull PDF.

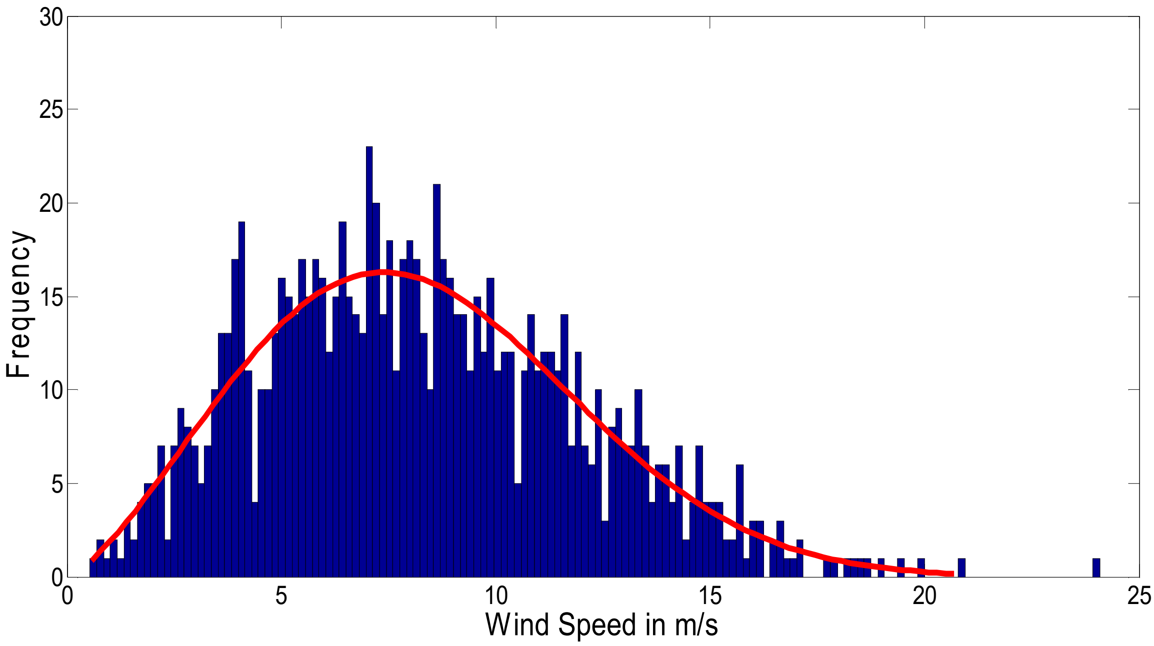

Figure 1. Wind speed probabilities.

The output power of a wind turbine can be planned as a function of the wind speed as follows [26]:

$$P_{\omega}(v_{\omega}) = \begin{cases} 0 \quad \text{for} \quad v_{\omega} < v_{\omega i}\,, \ v_{\omega} > v_{\omega o} \\ P_{\omega r}\left(\frac{v_{\omega} - v_{\omega i}}{v_{\omega r} - v_{\omega i}}\right) \ \text{for} \quad (v_{\omega i} \leq v_{\omega} \leq v_{\omega r}) \\ P_{\omega r} \quad \text{for} \quad (v_{\omega r} \leq v_{\omega} \leq v_{\omega o}) \end{cases} \tag{30}$$

where $P_{\omega r}$ is the rated output power of the WT, and $v_{\omega i}$ = 3 m/s, $v_{\omega o}$ = 25 m/s, and $v_{\omega r}$ = 16 m/s are the cut-in, cut-out, and rated speed of the wind turbine, respectively.

3.2. Modeling Solar Irradiance Uncertainty

The lognormal PDF can be used to model uncertainty in solar irradiation [27]:

$$f_G(G) = \frac{1}{G\,\sigma_s\sqrt{2\pi}} \exp\left[-\frac{(\ln G - \mu_s)^2}{2\,\sigma_s^2}\right] \text{for } G > 0 \tag{31}$$

where $\mu_{s,}$ and σ_s denote the mean and the standard deviation of random variables that were set at 5.5 and 0.5, respectively [27]. Figure 2 shows the solar irradiation scenarios generated by the Monte Carlo simulation.

The output power of a photovoltaic array as a function of solar irradiance can be calculated using the formula below [27]:

$$P_s(G) = \begin{cases} P_{sr}\left(\frac{G^2}{G_{std} \times M_c}\right) \text{for } 0 < G \leq M_c \\ P_{sr}\left(\frac{G}{G_{std}}\right) \text{for } G \geq M_c \end{cases} \tag{32}$$

where M_c stands for a specific irradiance point of 120 W/m^2, and G_{std} stands for standard solar irradiance, i.e., 1000 W/m^2.

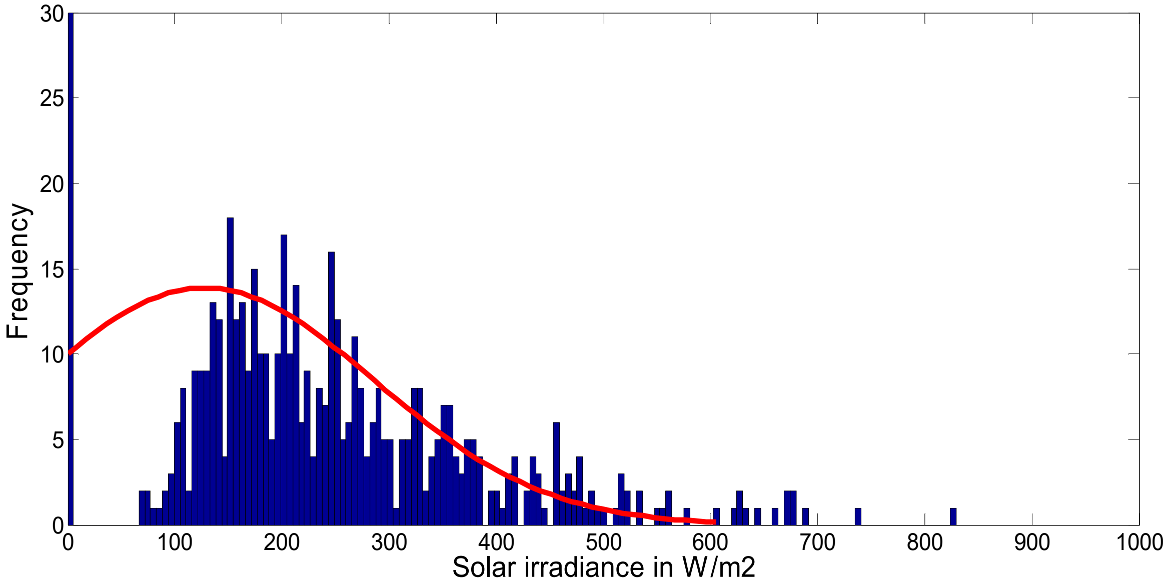

Figure 2. Solar irradiance probabilities.

3.3. Modeling Load Demand Uncertainty

The normal (PDF) is used to model the loading uncertainty [27]:

$$f_d(P_d) = \frac{1}{\sigma_d\sqrt{2\pi}} \exp\left[-\frac{(P_d - \mu_d)^2}{2{\sigma_d}^2}\right] \quad (33)$$

where the mean deviation and standard deviation values are μ_d and σ_d, respectively, and P_d is the load demand. Figure 3 shows the scenarios generated in the Monte Carlo simulation with σ_d = 10, μ_d = 70, and sample size 1000.

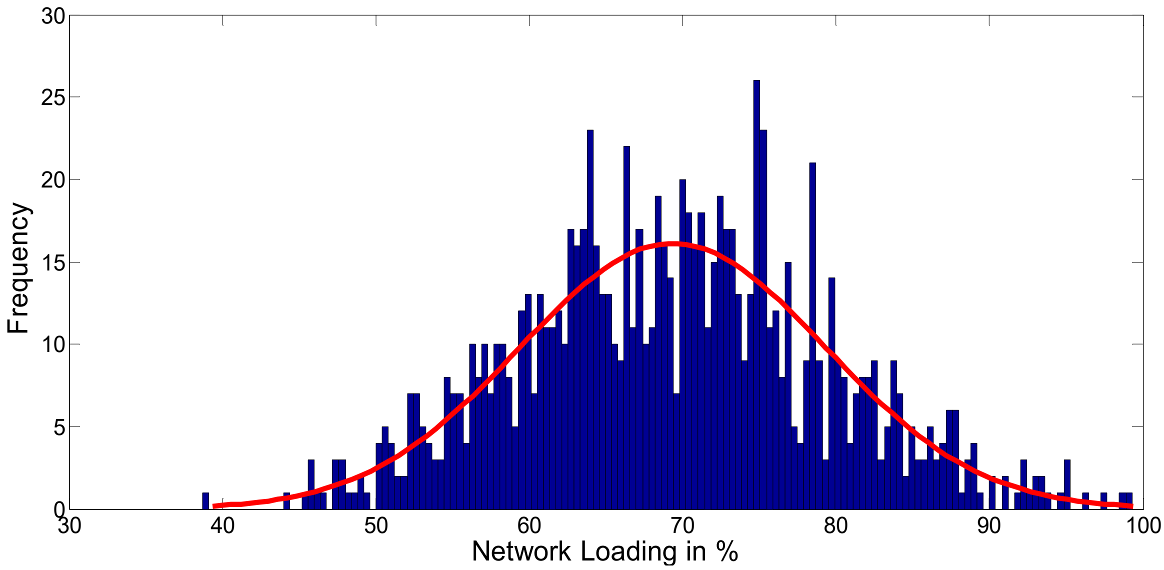

Figure 3. Load demand probabilities.

The backward reduction procedure can be used to reduce the number of the generated scenarios, as explained in [3]. Table 1 shows the generated scenarios and the corresponding loading, wind speed, and solar irradiance.

Table 1. The obtained scenarios, as well as the loading, wind speed, and solar irradiance.

Scenario No.	π_S	The Solar Irradiance (Watt/m^2)	The Wind Speed (m/s)	The Loading (%)
1	0.0070	521.47	5.46	62.84
2	0.0010	277.70	10.92	93.18
3	0.0220	472.83	4.92	62.95
4	0.0010	829.18	12.41	76.19
5	0.0010	604.47	9.38	73.18
6	0.0010	510.96	11.66	97.56
7	0.0010	577.89	3.466	72.75
8	0.0130	416.04	7.95	76.11
9	0.0010	737.85	7.41	75.58
10	0.0080	325.53	4.71	83.91
11	0.0060	674.26	4.01	69.22
12	0.0030	370.80	11.59	46.66
13	0.0020	167.32	6.31	47.29
14	0.1200	155.97	10.84	77.08
15	0.0100	229.79	7.15	59.75
16	0.0020	621.97	10.87	86.95
17	0.0030	632.85	5.98	67.12
18	0.0020	314.21	8.86	45.43
19	0.0370	338.70	7.09	64.45
20	0.0040	554.92	4.14	67.91
21	0.0060	138.20	9.94	50.69
22	0.0790	206.56	5.06	62.76
23	0.0240	378.86	3.89	75.36
24	0.0210	106.92	8.86	64.79
25	0.0080	73.166	5.81	63.62
26	0.0220	297.92	8.65	77.02
27	0.0080	232.25	11.07	87.02
28	0.0080	435.76	10.92	61.19
29	0.5100	0	9.91	69.88
30	0.0690	269.62	5.67	73.83

4. Gorilla Troops Optimizer (GTO)

GTO is a novel optimization technique proposed by Abdollahzadeh et al. in 2021 [23]; it simulates the social behavior and movements of gorillas in the wild. Gorillas are sociable animals that live in groups, known as troops. Each troop has a silverback gorilla as its leader; that individual makes important decisions and protects the troop, and all other troop members follow him. Young male gorillas, known as the black backs, are second in the troop hierarchy. Black backs also follow the silverback and provide backup protection for the group.

The GTO technique is similar to other optimization techniques built on exploration and exploitation phases. Exploration in GTO comprises three strategies: the first relies on the gorilla moving to unknown sites, while the second and the third are based on the movement of a gorilla toward another gorilla or toward a known location. The exploitation phase comprises two methodologies: the first is based on moving with the silver back while the second describes the motion of adult females. In this algorithm, the location of the gorilla is denoted as X, while the location of the silverback is denoted as GX. Imagine that a gorilla is trying to find better food resources. Thus, in the iterative process, GX is generated in each iteration and exchanged if another solution with a better value is obtained. As explained before, the exploration phase of the GTO is based on three strategies that can be mathematically formulated as follows:

$$GX(t+1) = \begin{cases} (UB - LB) \times R_1 + LB, \text{rand} < p \\ (R_2 - C) \times X_r(t) + L \times H, \text{rand} \geq 0.5 \\ X(i) - L \times (L \times (X(t) - GX_r(t)) + R_3 \times (X(t) - GX_r(t))), \text{rand} < 0.5 \end{cases} \quad (34)$$

where UB and LB represent the upper and lower bounds, R_1, R_2, and R_3 are random parameters within [0,1], GX indicates a candidate solution to be updated, t represents the current iteration, rand denotes a random value within [0,1], p is a predefined value within range [0,1], and GX_r and X_r denote solutions that have been randomly selected. The other operators in Equation (38) are as follows:

$$C = F \times \left(1 - \frac{t}{MaxIt}\right) \quad (35)$$

$$F = \cos(2 \times R_4) + 1 \quad (36)$$

$$L = C \times l \quad (37)$$

$$H = Z \times X(t) \quad (38)$$

$$Z = [-C, C] \quad (39)$$

where MaxIt is the maximum number of iterations and R_4 is a random number [0,1]. The value of l can be changed from -1 to 1. The exploitation phase in GTO is based on two strategies: the first is based on the troop's movements, i.e., following the silverback; the second is based on competition for adult females, where the males in the group fight each other when the silverback becomes weak or old. The transition between the two movements is based on C, as defined in Equation (39), and W, which is a predetermined value. If $C \geq W$, then the gorillas update their location by following the silverback, as follows:

$$GX(t+1) = L \times M \times (X(t) - X_{silverback}) + X(t) \quad (40)$$

$$M = \left(\left|\frac{1}{N}\sum_{i=1}^{N} GX_i(t)\right|^g\right)^{\frac{1}{g}} \quad (41)$$

$$g = 2^L \quad (42)$$

where $X_{silverback}$ denotes the location of the silverback gorilla. If C < W, then the locations of the gorillas are updated based on the competition for adult females, which can be expressed as follows:

$$GX(i) = X_{silverback} - (X_{silverback} \times Q - X(t) \times Q) \times A \quad (43)$$

$$Q = 2 \times r_5 - 1 \quad (44)$$

$$A = \beta \times E \quad (45)$$

$$E = \begin{cases} N_1, & \text{rand } \geq 0.5 \\ N_2, & \text{rand } < 0.5 \end{cases} \quad (46)$$

where Q mimics the impact force, r_5 refers to a random value within [0,1], and β is a predefined parameter. If rand ≥ 0.5, then the value of E will be equal to the random values in the normal distribution and the problem's dimensions; however, if rand is less than 0.5, then E will be a random value in the normal distribution. A flow chart of the application of GTO to determine the optimal sizing and placement of RDGs in RDNs is depicted in Figure 4.

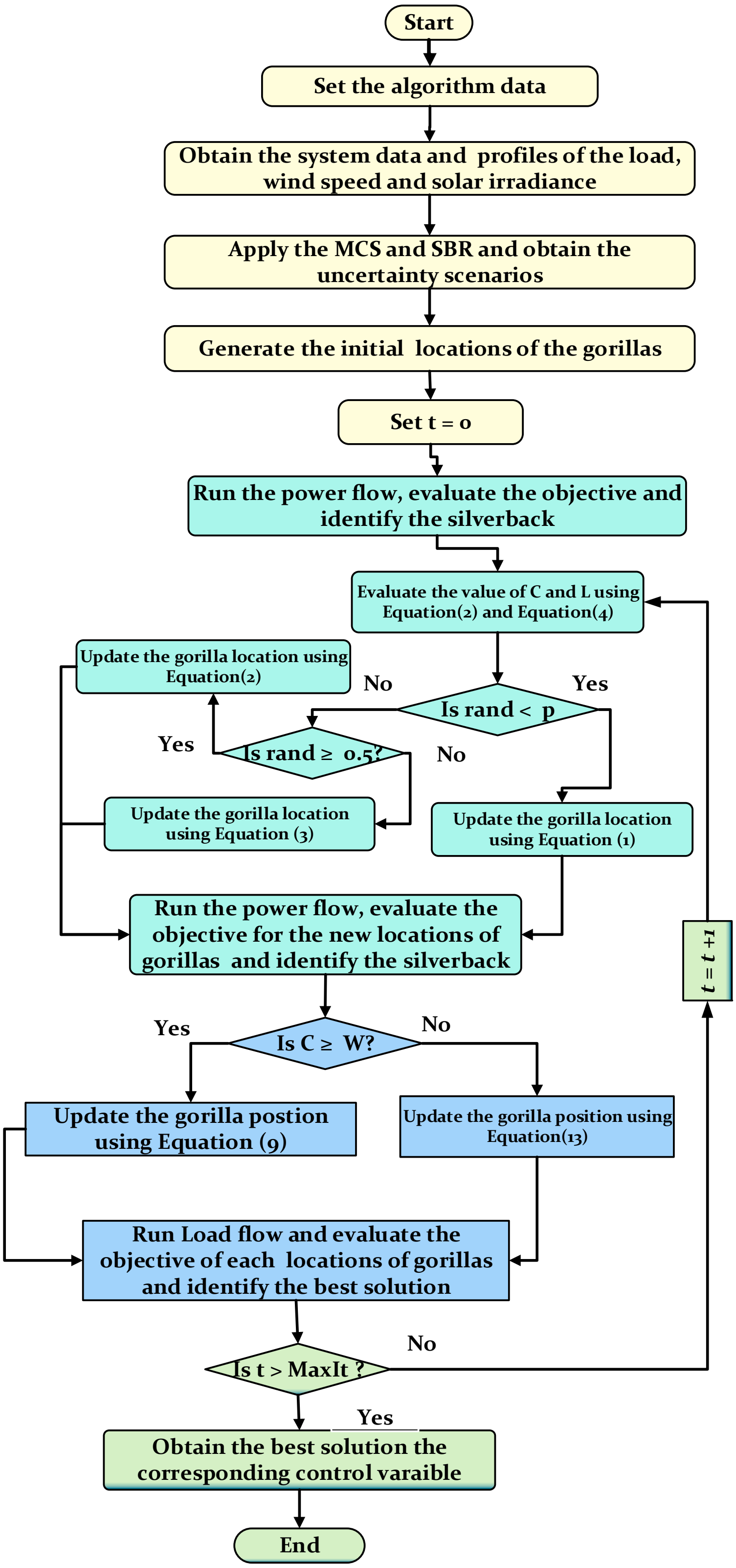

Figure 4. Flow chart of the GTO to determine the optimal RDGs in RDNs.

5. Simulation Results

The proposed GTO is used to identify the optimal RDGs in this section, and the proposed algorithm is used to determine the optimal RDG allocation in two RDNs, taking uncertainty in the system into consideration. RDGs are applied to reduce the expected total cost (ETCost), expected total emissions (ETEmission), and expected total voltage deviations (ETVD), and to maximize the expected total voltage stability index (ETVSI). The RDGs, including a solar PV unit, and WT-based DGs are incorporated into IEEE 69-bus and 30-bus EDN systems. Figures 5 and 6 show the 30-bus and IEEE 69-bus systems, respectively, and their branches and buses are described in [27]. Table 2 depicts the initial power flow of these systems in the simplest scenario. The results were compared with those obtained using particle swarm optimization (PSO) [28], the ant lion optimizer (ALO) [29], the whale optimization algorithm (WOA) [30], and the sine cosine algorithm (SCA) [31] to verify the effectiveness of the proposed GTO. Table 2 lists the parameters of the various aforementioned strategies. Table 3 provides a list of the limitations of the system. Table 4 shows the characteristics of the generation resources. The characteristics of the generation resources are shown in Table 5. The algorithms for handling the allocation problem were built in MATLAB 2014a on a PC with a 3.2 GHz I7-8700 CPU and 24 GB RAM. The following cases were investigated:

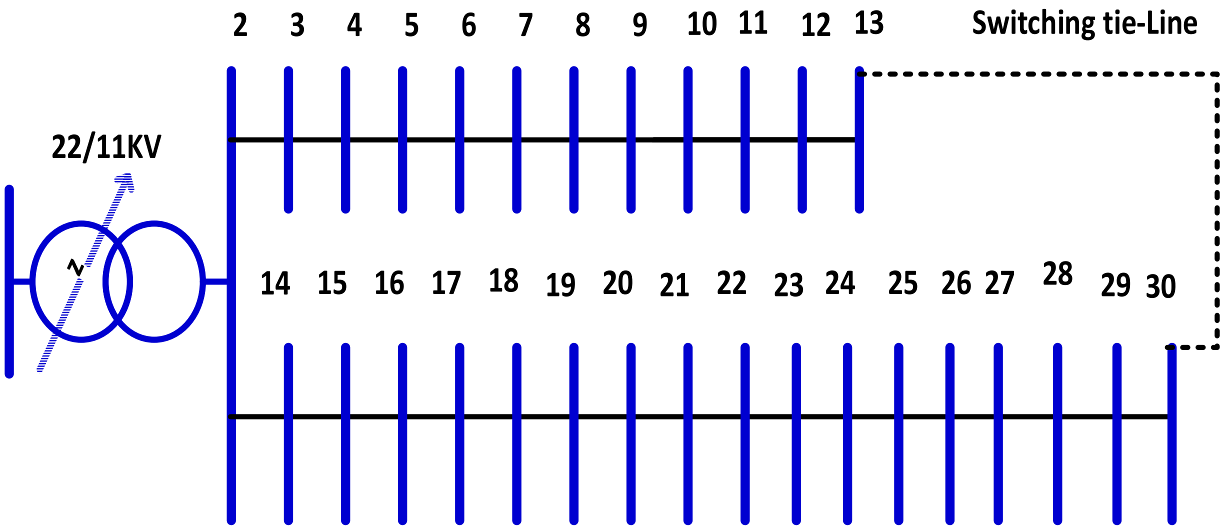

Figure 5. The EDN 30-bus system.

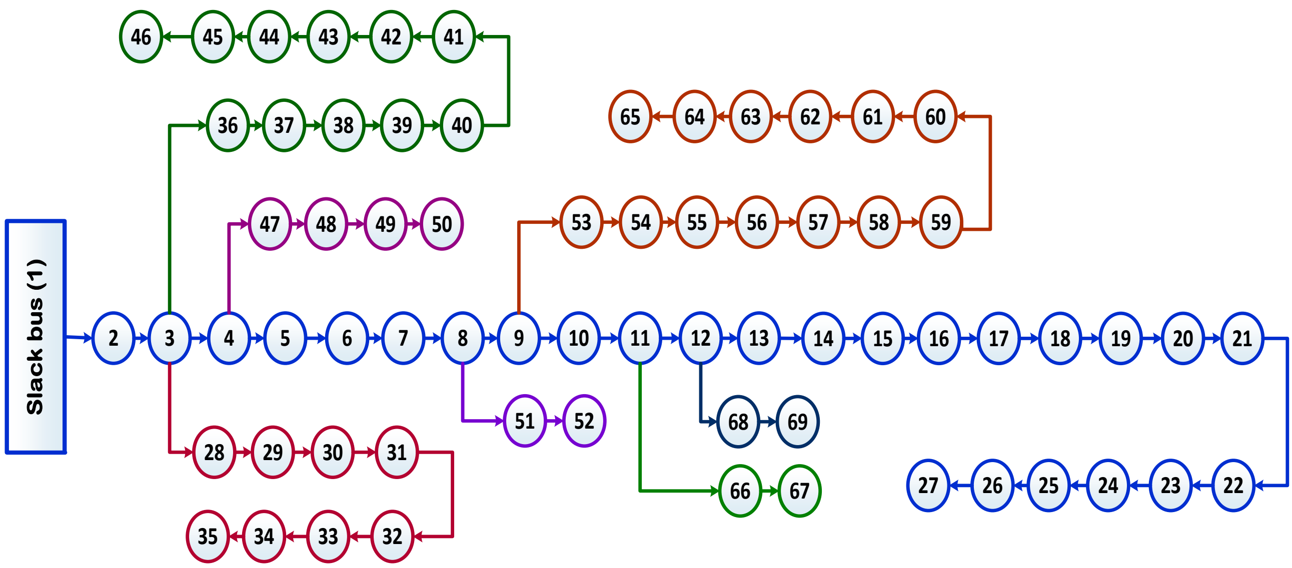

Figure 6. The IEEE 69-bus network.

Table 2. Specifications of the studied networks.

Item	30-Bus	69-Bus
V_{max} (p.u.)	0.9854 @ bus 2	0.9999 @ bus 2
V_{min} (p.u.)	0.9463 @ bus 30	0.9091 @ bus 65
Total reactive load (kVAR)	14,162.265	2694.600
Total active load (kW)	22,441.259	3801.49
Total reactive loss (kVAR)	361.184	102.187

Table 3. Applied parameters.

Optimizer	Parameter Configuration
GTO	Populations = 25, MaxIt = 100, $p = 0.03$; $\beta = 3$; w = 0.8
PSO [28]	Populations = 25, MaxIt = 100, w = 0.7, $b_1 = 2$, $b_2 = 1$
ALO [29]	Populations = 25, MaxIt = 100
WOA [30]	Populations = 25, MaxIt = 100
SCA [31]	Populations = 25, MaxIt = 100

Table 4. System limits.

Parameters	Values
Voltage limits	$1.05 \geq V_i \geq 0.90$ p.u.
Power factor limits	$0.65 \leq PF_i \leq 1$
Boundary of DG's size	$0 \leq P_{WT,\,PV} \leq P_L$ kW

Table 5. Generating resource characteristics.

DG Type	Fuel Cost ($/kWh)	Capital Cost ($/kW)	O&M Cost ($/kWh)	Life Time (Year)	Capacity Rate (MW)	Emission Factors (lb/MWh)
WT	-	1822	0.00952	20	5	-
Grid	0.044	-	-	25	25	5.06
PV	-	3985	0.01207	20	1	-

5.1. System of IEEE 69-Bus

In this case, by using GTO, the optimal sizes of the WT and solar PV were found to be 2826 kW and 975 kW, and their optimal sites were at buses 59 and 25, respectively. Without RDGs, the sums of ETCost, ETEmission, ETVD, and ETVSI were 269.78 USD/h, 5,754,400 kg/MWh, 0.14031 p.u., and 0.627188 p.u., respectively. With RDGs, the sums of ETCost, ETEmission, ETVD, and ETVSI were reduced to 193.4106 $/h, 2,742,900 kg/MWh, and 0.4637 p.u., respectively, while the voltage stability index increased to 66.4450 p. u. Table 6 depicts the probability of each scenario and the corresponding loading, PV and WT output powers, the ETCost, ETEmission, ETVD, and ETVSI. As shown in Table 6, the minimum expected emissions were observed under scenario 12. This was due to the high generated power from the WT- and PV-based DGs. The highest values for ETCost, ETEmission, and ETVD occurred in scenario 29, because the solar PV output power was zero kilowatts. Figures 7–10 show the cost, emissions, VD, and VSI for each scenario. Referring to these figures, it may be seen that ETCost, ETEmission, and ETVD were reduced considerably, while ETVSI was enhanced, through the inclusion of RDGs. The voltage profiles for each scenario without and with RDGs are shown in Figures 11 and 12, respectively. Table 7 summarizes the statistical findings of the objective function when various optimization strategies are used. From Table 7, it may be seen that GTO is superior to the PSO, WOA, SCA, and ALO techniques for solving this problem in terms of the mean, the worst, and the best values. In order to achieve a compromise between the best solution and a good run time, the parameters required to implement the proposed GTO were adjusted by running this algorithm 25 times; these parameters were the maximum number of iterations and of search agents, i.e., 60 and 15, respectively. For a fair comparison, the maximum number of iterations for all the applied technique was the same, i.e., 60.

Table 6. Generating resource characteristics.

Scenario No.	π_S	Loading (%)	P_w (kW)	P_s (kW)	ETCost (USD/h)	ETEmission (kg/MWh)	ETVD (p.u.)	ETVSI (p.u.)
1	0.0070	62.84	534.8	508.4332	1.3776	20,000	0.0034	0.4632
2	0.0010	93.18	1721.7	270.7575	0.2243	3300	0.0003	0.067
3	0.0220	62.95	417.4	461.0092	4.6716	71,000	0.0131	1.4452
4	0.0010	76.19	2045.6	808.4505	0.0927	300	0.0007	0.0705
5	0.0010	73.18	1386.9	589.3583	0.1523	1700	0.0002	0.0682
6	0.0010	97.56	1882.6	498.186	0.2082	2800	0.0001	0.0679
7	0.0010	72.75	101.3	563.4428	0.2724	4500	0.0009	0.0647
8	0.0130	76.11	1076.1	405.639	2.6652	38,400	0.0046	0.866
9	0.0010	75.58	958.7	719.4038	0.1879	2500	0.0004	0.0673
10	0.0080	83.91	371.7	317.3918	2.4663	42,500	0.0083	0.5123
11	0.0060	69.22	219.6	657.4035	1.4357	22,700	0.0042	0.3928
12	0.0030	46.66	1867.3	361.53	0.1093	0	0.0016	0.2103
13	0.0020	47.29	719.5	163.137	0.3016	3900	0.0008	0.1327
14	0.1200	77.08	1704.3	152.0708	21.1955	273,900	0.0366	8.0875
15	0.0100	59.75	902.1	224.0452	1.7519	24,000	0.0041	0.664
16	0.0020	86.95	1710.8	606.4208	0.3487	4200	0.0003	0.1368
17	0.0030	67.12	647.8	617.0288	0.5797	8200	0.0013	0.1998
18	0.0020	45.43	1273.9	306.3547	0.1679	700	0.0003	0.1368
19	0.0370	64.45	889.1	330.2325	6.8384	95,300	0.0144	2.4593
20	0.0040	67.91	247.8	541.047	0.9642	15,400	0.0029	0.2609
21	0.0060	50.69	1508.6	134.745	0.5876	3900	0.0016	0.4091
22	0.0790	62.76	447.8	201.396	18.2108	290,300	0.0623	5.131
23	0.0240	75.36	193.5	369.3885	6.941	118,400	0.0242	1.5398
24	0.0210	64.79	1273.9	92.8841	3.6211	48,200	0.0072	1.4007
25	0.0080	63.62	610.9	43.4953	1.8544	29,700	0.0065	0.5187
26	0.0220	77.02	1228.2	290.472	4.503	64,700	0.0078	1.4651
27	0.0080	87.02	1754.3	226.4438	1.6215	22,500	0.0022	0.5381
28	0.0080	61.19	1721.7	424.866	0.7579	3700	0.0026	0.5533
29	0.5100	69.88	1502.1	0	91.7617	1,240,800	0.1959	34.035
30	0.0690	73.83	580.4	262.8795	17.5402	285,400	0.0546	4.481
Summation	1				193.4106	2,742,900	0.4637	66.445

Table 7. The statistical results of using different optimizers in the IEEE 69-bus system.

Optimizer	Best	Average	Worst	Deviation from the Mean	Elapsed Time (s)
GTO	0.6419	0.6657	0.7057	0.0201	108
PSO [28]	0.6847	0.7838	0.9178	0.0565	95.3
ALO [29]	0.6474	0.7614	0.8712	0.0631	97
WOA [30]	0.6699	0.7290	0.7978	0.0424	95.1
SCA [31]	0.6654	0.6883	0.7189	0.0159	95

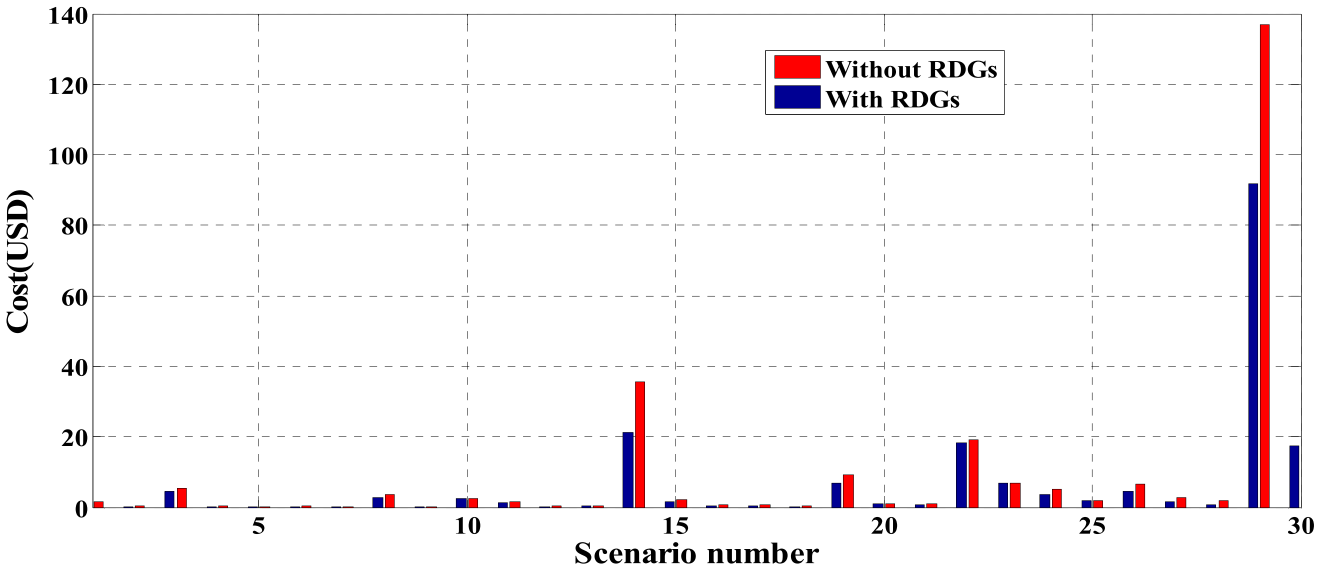

Figure 7. Total cost of each 69-bus system scenario.

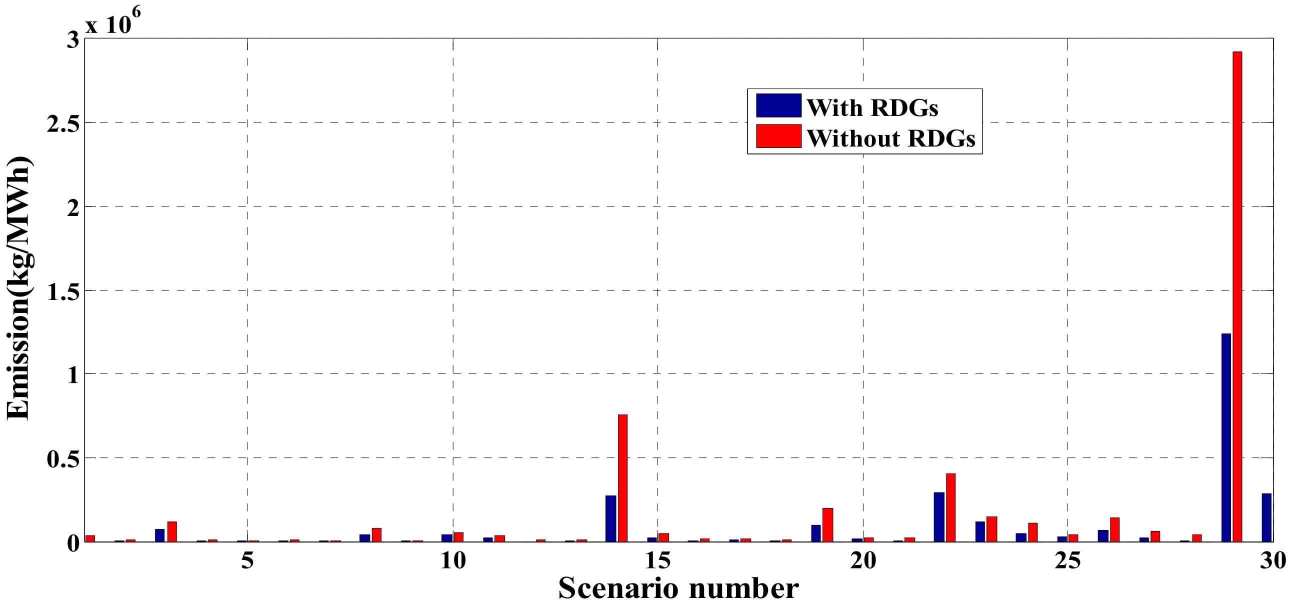

Figure 8. Total emissions of each 69-bus system scenario.

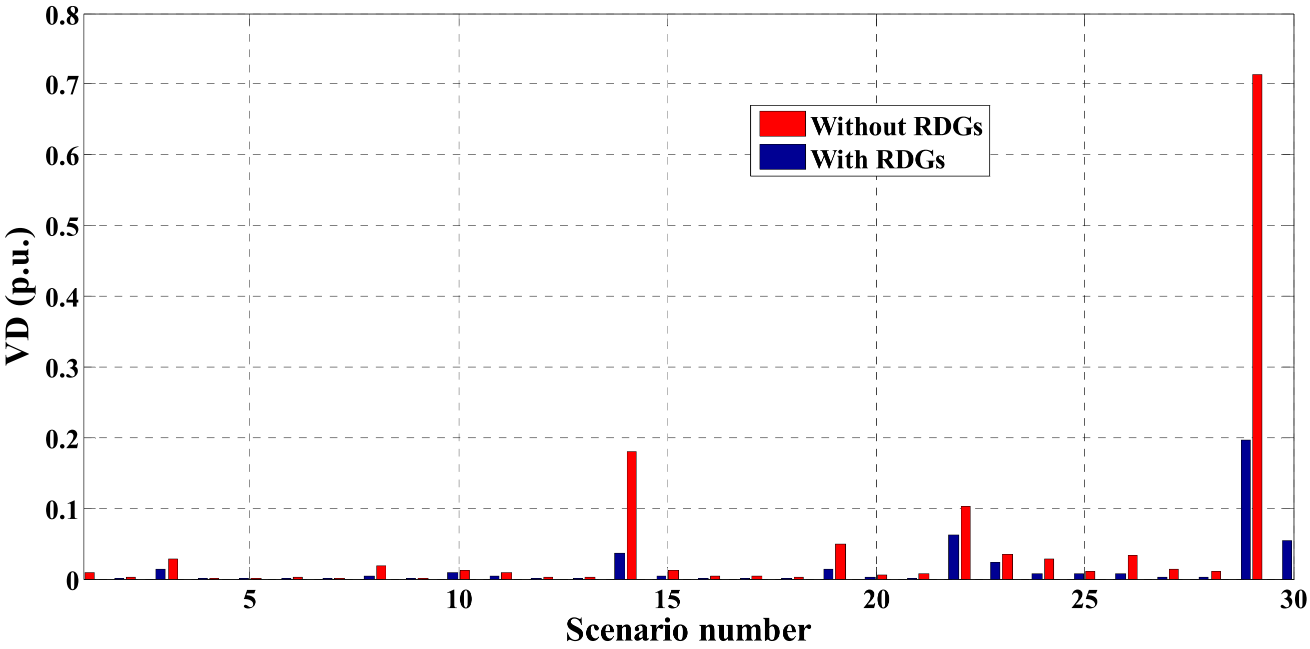

Figure 9. Total VDs of each 69-bus system scenario.

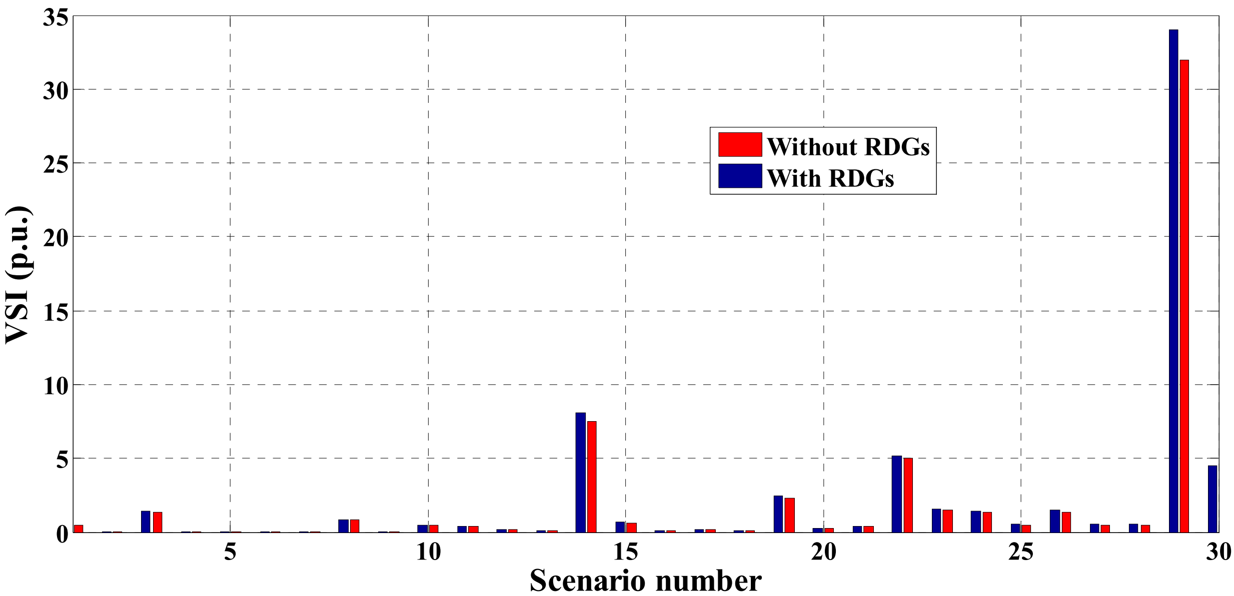

Figure 10. Total VSIs of each 69-bus system scenario.

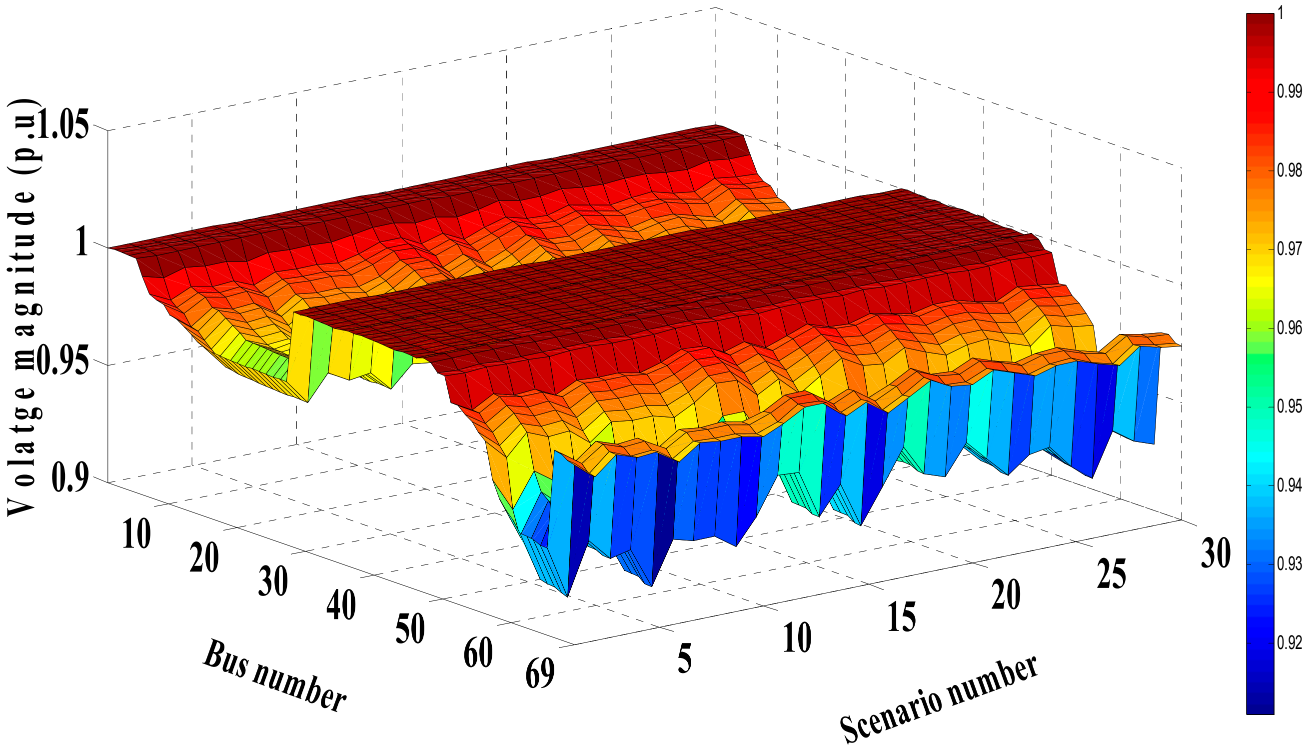

Figure 11. Magnitudes of the IEEE 69-bus system voltage bus without RDGs.

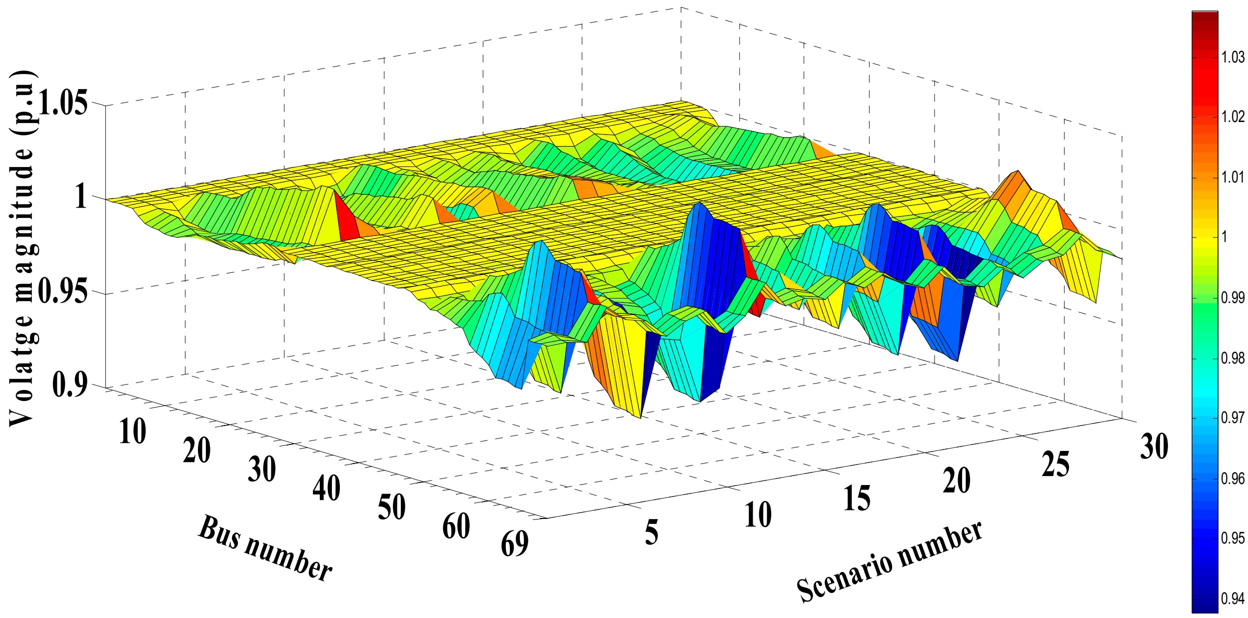

Figure 12. Magnitudes of the IEEE 69-bus system voltage bus with RDGs.

5.2. The EDN 30-Bus System

GTO was applied to allocate RDGs in an EDN 30-bus network. The optimal placements of PV and WT were at buses 30 and 17, while their optimal ratings were 5000 kW and 17,440 kW, respectively. Without RDGs, the total ETCost, ETEmission, ETVD, and ETVSI were 1492.9 USD/h, 31,844,000 kg/MWh, 0.7851 p.u., and 25.9978 p.u., respectively. With optimal inclusion of RDGs, ETCost, ETEmission, ETVD, and ETVSI decreased to 1105.2 $/h, 15,571,000 kg/MWh, 0.2571 p.u., and 28.1776 p.u., respectively, representing improvements of 25.97% and 51.1%, 67.25%, and 7.7%.

Table 8 lists the probability of each scenario and the corresponding loading, PV and WT output powers, ETCost, ETEmission, ETVD, and ETVSI. As seen in Table 6, it is clear that the minimum expected cost and emission occurs in scenario 12. This was due to the high generated power from WT- and PV-based DGs. In addition, the highest values for ETCost, ETEmission, and ETVD occur in scenario 29, because the solar PV output power was 0 kW.

Table 8. Simulation results of EDN 30-bus network.

Scenario No.	π_s	Loading (%)	P_w (kW)	P_s (kW)	ETCost (USD/h)	ETEmission (kg/MWh)	ETVD (p.u.)	ETVSI (p.u.)
1	0.0070	62.84	3300	2607.3	8.1310	120,000	0.0021	0.1949
2	0.0010	93.18	10,626	1388.5	1.2894	18,700	0.0002	0.0285
3	0.0220	62.95	2576	2364.1	27.4925	423,000	0.0081	0.6064
4	0.0010	76.19	12,625	4145.9	0.5393	1600	0.0005	0.0305
5	0.0010	73.18	8560	3022.4	0.8952	10,300	0.0003	0.0291
6	0.0010	97.56	11,618	2554.8	1.2058	16,400	0.0003	0.0290
7	0.0010	72.75	625	2889.5	1.6008	27,000	0.0005	0.0269
8	0.0130	76.11	6641	2080.2	15.5925	226,300	0.0028	0.3662
9	0.0010	75.58	5917	3689.2	1.1188	15,400	0.0002	0.0285
10	0.0080	83.91	2294	1627.6	14.3988	249,700	0.0050	0.2128
11	0.0060	69.22	1355	3371.3	8.4888	136,400	0.0025	0.1641
12	0.0030	46.66	11,524	1854	0.5371	0	0.0013	0.0912
13	0.0020	47.29	4441	836.6	1.7394	22,300	0.0005	0.0562
14	0.1200	77.08	10,518	779.9	119.9752	1,523,300	0.0261	3.4526
15	0.0100	59.75	5568	1149	10.1495	139,300	0.0023	0.2810
16	0.0020	86.95	10,559	3109.8	2.0374	25,000	0.0007	0.0584
17	0.0030	67.12	3998	3164.3	3.4395	49,600	0.0008	0.0842
18	0.0020	45.43	7862	1571.1	0.9497	3700	0.0005	0.0586
19	0.0370	64.45	5487	1693.5	39.9085	561,000	0.0084	1.0397
20	0.0040	67.91	1529	2774.6	5.6792	91,900	0.0018	0.1090
21	0.0060	50.69	9311	691	3.2320	18,800	0.0015	0.1756
22	0.0790	62.76	2764	1032.8	105.9559	1,697,400	0.0363	2.1491
23	0.0240	75.36	1194	1894.3	40.5638	696,600	0.0145	0.6396
24	0.0210	64.79	7862	476.3	20.6340	271,800	0.0037	0.5953
25	0.0080	63.62	3770	223.1	10.7080	171,500	0.0037	0.2176
26	0.0220	77.02	7580	1489.6	26.1219	376,400	0.0045	0.6205
27	0.0080	87.02	10,827	1161.2	9.2621	127,200	0.0018	0.2293
28	0.0080	61.19	10,626	2178.8	4.2792	19,200	0.0030	0.2382
29	0.5100	69.88	9271	0	516.9923	6,857,100	0.0909	14.4896
30	0.0690	73.83	3582	1348.1	102.3210	1,674,000	0.0322	1.8752
Summation	1				1105.2	15,571,000	0.2571	28.1776

Figures 13–16 show the cost, emissions, VD, and VSI for each scenario. Referring to these figures, the cost, emission, and VD were reduced considerably while VSI increased with the optimal placement of RDGs. Figures 17 and 18 show the voltage profiles without and with RDGs, respectively. It clear that the system voltage was boosted with the inclusion of RDGs. Table 9 presents statistical results obtained using various optimization methods. It is clear that GTO is superior to the WOA, PSO, SCA, and ALO techniques for this problem in terms of the mean, the worst, and the best values.

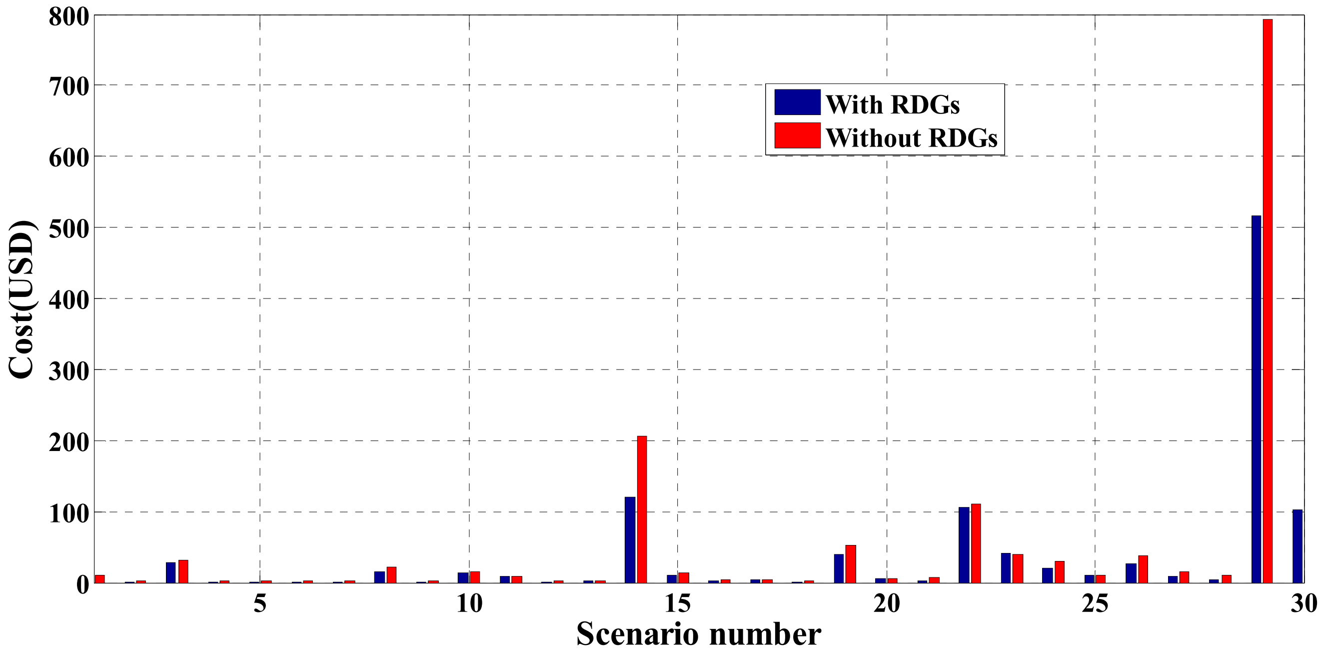

Figure 13. Total cost for each 30-bus system scenario.

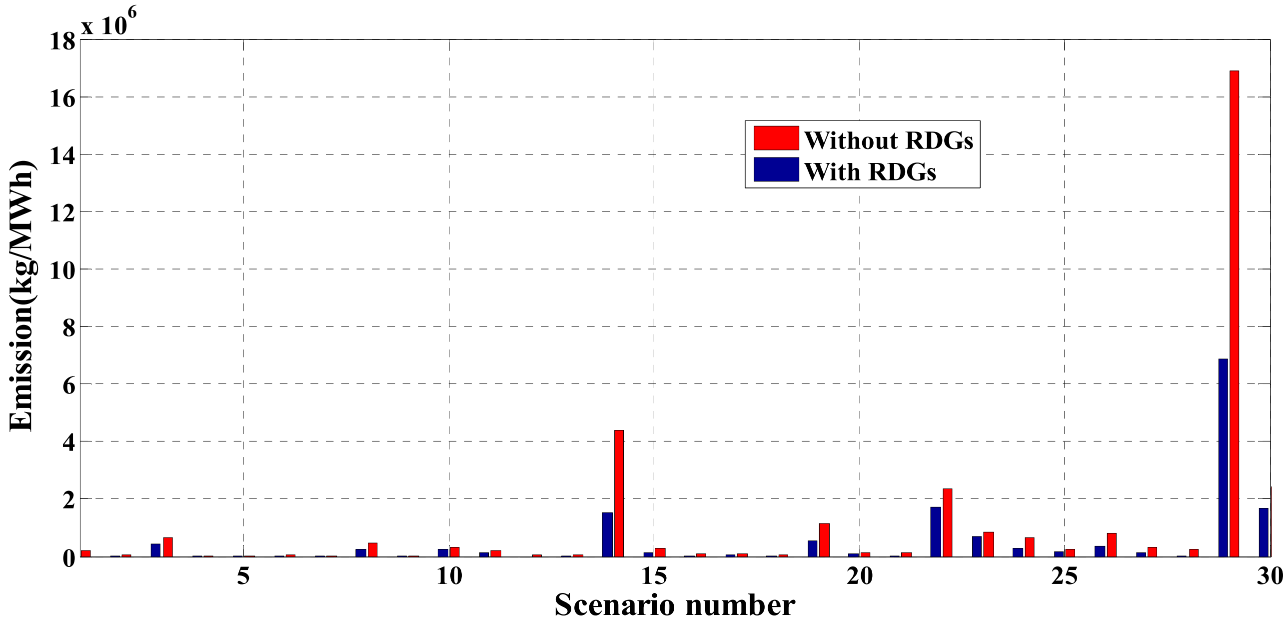

Figure 14. Total emissions for each 30-bus system scenario.

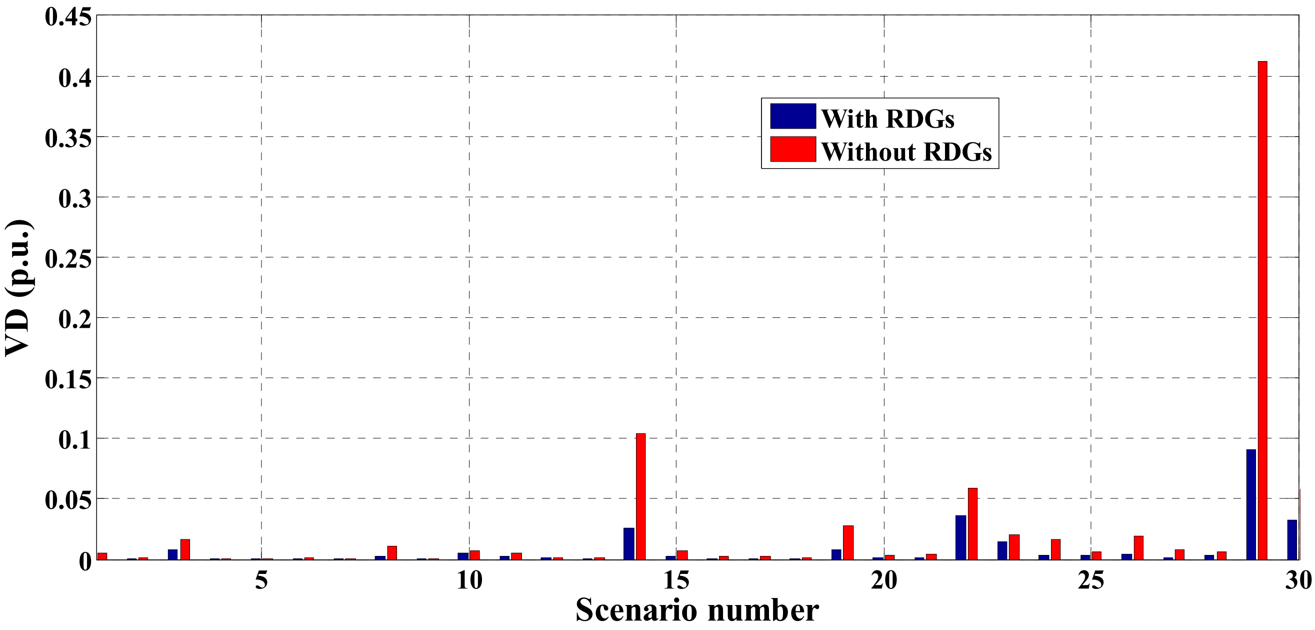

Figure 15. Total VDs for each 30-bus system scenario.

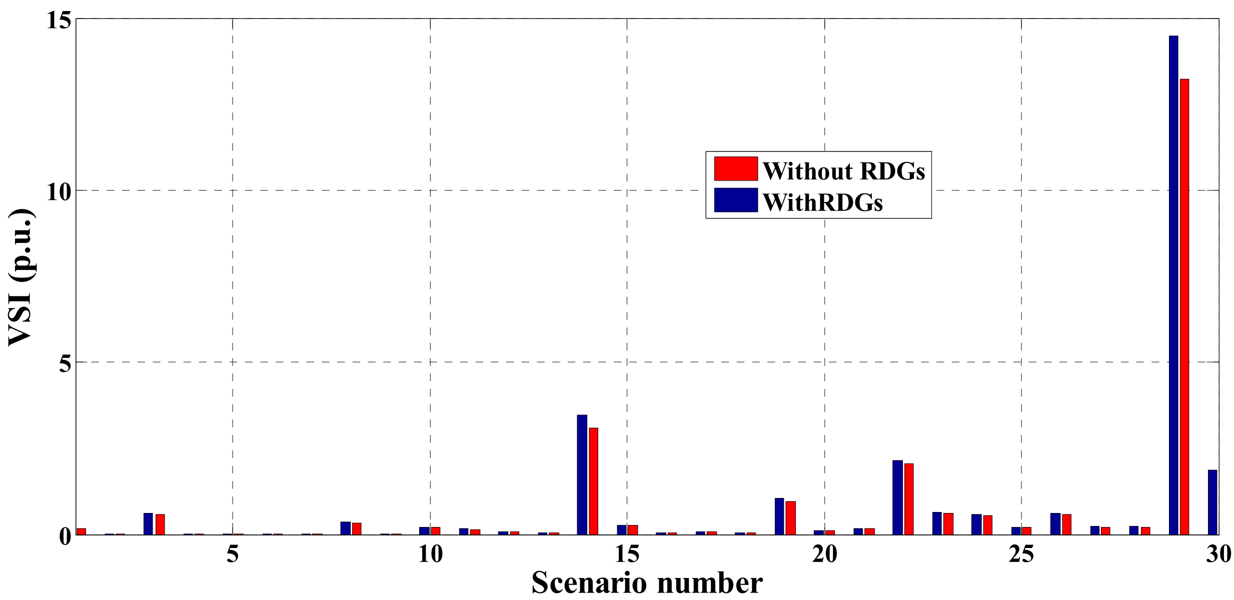

Figure 16. Total VSIs for each 30-bus system scenario.

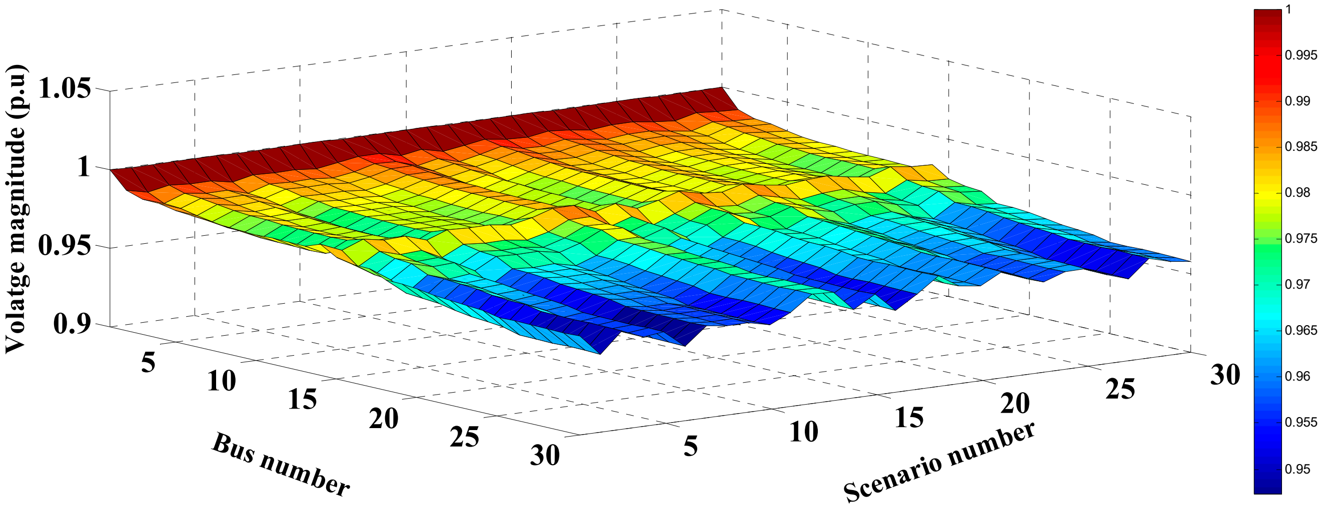

Figure 17. The voltage profile of the 30-bus network without RDGs.

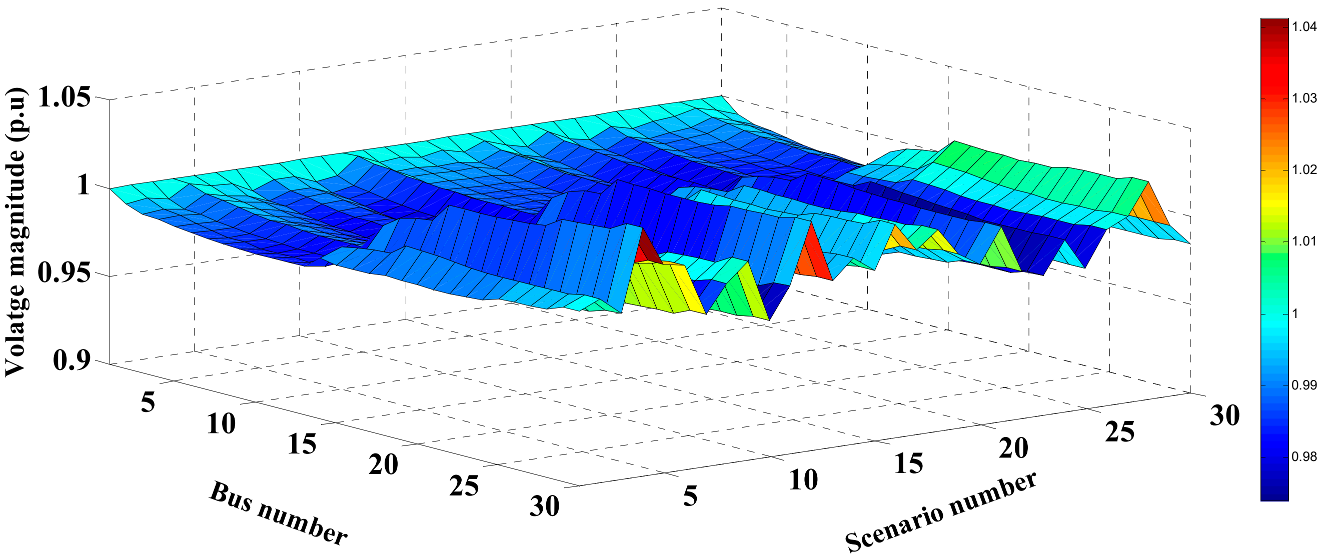

Figure 18. The voltage profile of the 30-bus network with RDGs.

Table 9. Statistical results of using different optimizers in the EDN 30-bus system.

Optimizer	Best	Average	Worst	Deviation from the Mean	Elapsed Time (s)
GTO	0.6454	0.6536	0.7130	0.0182	47
PSO [28]	0.6670	0.7181	0.8103	0.0344	34
ALO [29]	0.6576	0.7003	0.7817	0.0348	38.2
WOA [30]	0.6519	0.7011	0.7728	0.0334	38
SCA [31]	0.6524	0.6687	0.6845	0.0102	35

6. Conclusions

This paper presents an efficient optimizer, named the gorilla troops optimizer (GTO), which may be used to determine the optimal sizes and sites of RDGs, including WT- and PV-based generation units, in a distribution system for a multiobjective function, including reducing total costs, emissions, and voltage deviations, and enhancing system stability. The allocation problem of RDGs was addressed taking the uncertainties of loading and the output power of the RDGs into account. The lognormal PDF, the normal PDF, and

Weibull PDF were used to represent the uncertainties of solar irradiance, loading, and wind speed, respectively. In addition, a Monte Carlo simulation was applied to generate a set of scenarios (1000 scenarios). This set was reduced to just 30 scenarios using the backward reduction method. The allocation problem was solved for two radial distribution networks: an IEEE 69-bus and a real EDN 30-bus distribution system in Egypt. From the obtained results, the main findings are as follows:

1. In the IEEE 69-bus, through the optimal integration of RDGs, the expected total cost, emissions, summation of voltage deviations, and voltage stability index were reduced by 28.3%, 52.34%, and 66.95%, respectively, and the stability of the system was enhanced by 5.6%, compared to the base case.
2. In the EDN 30-bus network, the expected total costs, emissions, and summation of the voltage deviations were reduced by 25.97%, 51.1%, and 67.25%, respectively, and the stability of the system was enhanced by 7.7%, compared to the base case.
3. The proposed algorithm is superior to the PSO, WOA, ALO, and SCA techniques for deterministic and probabilistic solutions to the RDGs allocation problem.

Author Contributions: Conceptualization, M.E. and S.K.; Data curation, M.E. and S.K.; Formal analysis, M.E. and S.K.; Funding acquisition, S.K., A.M.A. and M.T.-V.; Investigation, A.R. and M.E.; Methodology, A.R. and M.E.; Project administration, S.K., A.M.A. and M.T.-V.; Resources, S.K., A.M.A. and M.T.-V.; Software, S.K. and A.M.A.; Supervision, M.E., S.K. and M.T.-V.; Validation, M.E. and S.K.; Visualization, A.M.A. and M.T.-V.; Writing—original draft, A.R. and M.E.; Writing—review and editing, S.K., A.M.A. and M.T.-V. All authors have read and agreed to the published version of the manuscript.

Funding: This research was funded by the Deputyship for Research & Innovation, Ministry of Education in Saudi Arabia through the project number "IF_2020_NBU_402".

Institutional Review Board Statement: Not Applicable.

Informed Consent Statement: Not Applicable.

Data Availability Statement: Not Applicable.

Acknowledgments: The authors extend their appreciation to the Deputyship for Research & Innovation, Ministry of Education in Saudi Arabia for funding this research work through the project number "IF_2020_NBU_402". The authors gratefully thank the Prince Faisal bin Khalid bin Sultan Research Chair in Renewable Energy Studies and Applications (PFCRE) at Northern Border University for their support and assistance.

Conflicts of Interest: The authors declare no conflict of interest.

References

1. Khuan, N.; Rahim, S.R.A.; Hussain, M.H.; Azmi, A.; Azmi, S.A. Integration of distributed generation and compensating capacitor in radial distribution system via firefly algorithm. Indones. *J. Electr. Eng. Comput. Sci.* **2019**, *16*, 67–73.
2. Iweh, C.D.; Gyamfi, S.; Tanyi, E.; Effah-Donyina, E. Distributed Generation and Renewable Energy Integration into the Grid: Prerequisites, Push Factors, Practical Options, Issues and Merits. *Energies* **2021**, *14*, 5375. [CrossRef]
3. Hemeida, M.G.; Alkhalaf, S.; Senjyu, T.; Ibrahim, A.; Ahmed, M.; Bahaa-Eldin, A.M. Optimal probabilistic location of DGs using Monte Carlo simulation based different bio-inspired algorithms. *Ain Shams Eng. J.* **2021**, *12*, 2735–2762. [CrossRef]
4. Kalajahi, S.M.S.; Baghali, S.; Khalili, T.; Mohammadi-Ivatloo, B.; Bidram, A. Multi-Objective Approach for Optimal Size and Location of DGs in Distribution Systems. In Proceedings of the 2020 IEEE Green Energy and Smart Systems Conference (IGESSC), Long Beach, CA, USA, 2–3 November 2020; pp. 1–6.
5. Devineni, G.K.; Ganesh, A.; Rao, D.N.M.; Saravanan, S. Optimal Sizing and Placement of DGs to Reduce the Fuel Cost and T& D Losses by using GA & PSO optimization Algorithms. In Proceedings of the 2021 International Conference on Sustainable Energy and Future Electric Transportation (SEFET), Hyderabad, India, 21–23 January 2021; pp. 1–6.
6. Ali, A.; Keerio, M.U.; Laghari, J.A. Optimal Site and Size of Distributed Generation Allocation in Radial Distribution Network Using Multi-objective Optimization. *J. Mod. Power Syst. Clean Energy* **2021**, *9*, 404–415. [CrossRef]
7. Weckx, S.; D'Hulst, R.; Driesen, J. Locational Pricing to Mitigate Voltage Problems Caused by High PV Penetration. *Energies* **2015**, *8*, 4607–4628. [CrossRef]
8. Georgilakis, P.S.; Hatziargyriou, N.D. A review of power distribution planning in the modern power systems era: Models, methods and future research. *Electr. Power Syst. Res.* **2015**, *121*, 89–100. [CrossRef]

9. Pandey, A.K.; Kirmani, S. Multi-objective optimal location and sizing of hybrid photovoltaic system in distribution systems using crow search algorithm. *Int. J. Renew. Energy Res.* **2019**, *9*, 1681–1693.
10. Selim, A.; Kamel, S.; Mohamed, A.; Elattar, E. Optimal Allocation of Multiple Types of Distributed Generations in Radial Distribution Systems Using a Hybrid Technique. *Sustainability* **2021**, *13*, 6644. [CrossRef]
11. Liu, Z.; Wen, F.; Ledwich, G. Optimal Siting and Sizing of Distributed Generators in Distribution Systems Considering Uncertainties. *IEEE Trans. Power Deliv.* **2011**, *26*, 2541–2551. [CrossRef]
12. Rathore, A.; Patidar, N. Optimal sizing and allocation of renewable based distribution generation with gravity energy storage considering stochastic nature using particle swarm optimization in radial distribution network. *J. Energy Storage* **2021**, *35*, 102282. [CrossRef]
13. Zeng, B.; Zhang, J.; Zhang, Y.; Yang, X.; Dong, J.; Liu, W. Active Distribution System Planning for Low-carbon Objective using Cuckoo Search Algorithm. *J. Electr. Eng. Technol.* **2014**, *9*, 433–440. [CrossRef]
14. Ahmed, D.; Ebeed, M.; Ali, A.; Alghamdi, A.; Kamel, S. Multi-Objective Energy Management of a Micro-Grid Considering Stochastic Nature of Load and Renewable Energy Resources. *Electronics* **2021**, *10*, 403. [CrossRef]
15. Biswal, S.R.; Shankar, G. Simultaneous optimal allocation and sizing of DGs and capacitors in radial distribution systems using SPEA2 considering load uncertainty. *IET Gener. Transm. Distrib.* **2019**, *14*, 494–505. [CrossRef]
16. Saric, M.; Hivziefendic, J.; Tesanovic, M. Optimal DG allocation for power loss reduction considering load and generation uncertainties. In Proceedings of the 2019 11th International Symposium on Advanced Topics in Electrical Engineering (ATEE), Bucharest, Romania, 28–30 March 2019; pp. 1–6.
17. Hadidian-Moghaddam, M.J.; Nowdeh, S.A.; Bigdeli, M.; Azizian, D. A multi-objective optimal sizing and siting of distributed generation using ant lion optimization technique. *Ain Shams Eng. J.* **2018**, *9*, 2101–2109. [CrossRef]
18. Ahmed, A.; Nadeem, M.F.; Sajjad, I.A.; Bo, R.; Khan, I.A.; Raza, A. Probabilistic generation model for optimal allocation of wind DG in distribution systems with time varying load models. *Sustain. Energy, Grids Netw.* **2020**, *22*, 100358. [CrossRef]
19. Eberhart, R.; Kennedy, J. A New Optimizer Using Particle Swarm Theory. In Proceedings of the Sixth International Symposium on Micro Machine and Human Science (MHS'95), Nagoya, Japan, 4–6 October 1995; pp. 39–43.
20. Abdel-Fatah, S.; Ebeed, M.; Kamel, S. Optimal reactive power dispatch using modified sine cosine algorithm. In Proceedings of the 2019 International Conference on Innovative Trends in Computer Engineering (ITCE), Aswan, Egypt, 2–4 February 2019; pp. 510–514.
21. Sakr, W.S.; El-Sehiemy, R.; Azmy, A.M. Adaptive differential evolution algorithm for efficient reactive power management. *Appl. Soft Comput.* **2017**, *53*, 336–351. [CrossRef]
22. Zhao, W.; Wang, L.; Mirjalili, S. Artificial hummingbird algorithm: A new bio-inspired optimizer with its engineering applications. Comput. *Methods Appl. Mech. Eng.* **2021**, *388*, 114194. [CrossRef]
23. Abdollahzadeh, B.; Gharehchopogh, F.S.; Mirjalili, S. Artificial gorilla troops optimizer: A new nature-inspired metaheuristic algorithm for global optimization problems. *Int. J. Intell. Syst.* **2021**, *36*, 5887–5958. [CrossRef]
24. Ginidi, A.; Ghoneim, S.M.; Elsayed, A.; El-Sehiemy, R.; Shaheen, A.; El-Fergany, A. Gorilla Troops Optimizer for Electrically Based Single and Double-Diode Models of Solar Photovoltaic Systems. *Sustainability* **2021**, *13*, 9459. [CrossRef]
25. El-Ela, A.A.A.; El-Sehiemy, R.A.; Abbas, A.S. Optimal Placement and Sizing of Distributed Generation and Capacitor Banks in Distribution Systems Using Water Cycle Algorithm. *IEEE Syst. J.* **2018**, *12*, 3629–3636. [CrossRef]
26. Mohseni-Bonab, S.M.; Rabiee, A. Optimal reactive power dispatch: A review, and a new stochastic voltage stability constrained multi-objective model at the presence of uncertain wind power generation. *IET Gener. Transm. Distrib.* **2017**, *11*, 815–829. [CrossRef]
27. Kamel, S.; Ramadan, A.; Ebeed, M.; Nasrat, L.; Ahmed, M.H. Sizing and evaluation analysis of hybrid solar-wind distributed generations in real distribution network considering the uncertainty. In Proceedings of the 2019 International Conference on Computer, Control, Electrical, and Electronics Engineering (ICCCEEE), Khartoum, Sudan, 21–23 September 2019; pp. 1–5.
28. Poli, R.; Kennedy, J.; Blackwell, T. Particle swarm optimization. *Swarm Intell.* **2007**, *1*, 33–57. [CrossRef]
29. Mirjalili, S. The ant lion optimizer. *Adv. Eng. Softw.* **2015**, *83*, 80–98. [CrossRef]
30. Mirjalili, S.; Lewis, A. The whale optimization algorithm. *Adv. Eng. Softw.* **2016**, *95*, 51–67. [CrossRef]
31. Mirjalili, S. SCA: A Sine Cosine Algorithm for solving optimization problems. *Knowl.-Based Syst.* **2016**, *96*, 120–133. [CrossRef]